

Dynamic output feedback control of systems with event-driven control inputs

Jinhui ZHANG*, Hao XU, Li DAI & Yuanqing XIA

School of Automation, Beijing Institute of Technology, Beijing 100081, China

Received 19 April 2019/Revised 27 June 2019/Accepted 16 September 2019/Published online 16 March 2020

Abstract In this paper, a dynamic output feedback control problem is investigated for systems with event-driven control inputs. With both continuous and sampled output measurements in the systems, two types of dynamic output feedback controllers are designed based on a predefined event-driven scheduler for the control signals, respectively. With the proposed event-driven control scheme, the Zeno behavior can be avoided, and the states of closed-loop systems are also guaranteed to be globally uniformly ultimately bounded. Detailed parameters of the event-driven controllers are constructed under the stabilizable conditions of the closed-loop systems. Finally, both the effectiveness and merits of the proposed design techniques are verified by the numerical examples.

Keywords networked control systems, NCSs, event-driven control, dynamic output feedback control

Citation Zhang J H, Xu H, Dai L, et al. Dynamic output feedback control of systems with event-driven control inputs. *Sci China Inf Sci*, 2020, 63(5): 150202, <https://doi.org/10.1007/s11432-019-2659-3>

1 Introduction

In many industrial control applications, such as manufacturing plants, power plants, automobiles, aircrafts, and robot manipulators, networks have played important roles for the rapid development of computer and communication technologies [1–3]. Especially in some engineering applications, measurements and control signals are exchanged among spatially distributed system components by networks [4–6]. In this situation, the traditional control systems have been evolved to networked control systems (NCSs). As shown in [7–9], there exist many advantages of NCSs such as low cost, simple installation and maintenance, reduced weight and power requirements as well as high reliability comparing with traditional feedback control systems.

In NCSs, network communication constraints, e.g., networked data dropouts and induced delays, make a great influence on the control performance of NCSs [10–13]. In order to attenuate the negative effects of the network communication constraints, it is feasible to save the usage of communication resources while maintaining the system performance at a good level. Based on an idea of that the control inputs are updated or transmitted only when the chosen error signals exceeding a designed threshold, the event-driven control (is also called as event-triggered control) approach is proved to be an effective manner to reduce the utilization of the communication networks in theory and applications, which has attracted many scholars to do relative researches in recent years (please refer to [14–18]). Moreover, to produce the continuous-time input signal, a zero-order-holder (ZOH) is always implemented in the event-driven control systems. It is worth considering that, for many practical applications, the full state information

* Corresponding author (email: zhangjinh@bit.edu.cn)

is not always available, and only the output is accessible. But in [14–17], the assumption is provided in the developed event-driven approaches that all the internal plant states are available to the control law. One solution to address this problem is to use a state observer to reconstruct the system states. It should be pointed out that the reconstruction of system states requires to obtain the current inputs of plants at the controller sides [19]. In NCSs, owing to the distributive location of controller and actuator, and data dropouts and time-varying network communication delays in the controller-to-actuator channel, the current inputs of plants are complicated and challenging to acquire at the controller sides. Alternatively, the dynamic output feedback (DOF) control strategies can be employed in which the control law only requires knowledge of measured output [20–22]. Especially, it is practicable and effective for most of NCSs in engineering to obtain reliable stabilisation with the information of dynamic observers from the designed DOF controller [23, 24].

In this paper, we pay attentions to the construction of DOF controllers for the systems with event-driven control inputs, and both the event-driven schedulers and the DOF controller parameters are determined for systems with continuous and sampled output measurements, respectively. By utilizing the designed controllers, transmission frequencies of control signals are significantly reduced in the communication channels, and the closed-loop control systems are guaranteed to satisfy the uniform ultimate bounded stability. Moreover, the Zeno behavior can be avoided because the minimum inter-scheduling interval between two consecutive transmitting instants is shown to be lower bounded by a positive scalar. Furthermore, the proposed DOF control schemes are applied to a linearized satellite system model, which shows that the proposed method significantly reduces the updating frequency of the controller while guarantees a certain performance of the control system in this simulation. The main contributions are highlighted as follows:

(1) For the continuous-time control systems with both continuous and sampled output measurements, two types of DOF controllers are designed, and two predefined event-driven schedulers are also proposed by using the control signals, respectively.

(2) Under the proposed event-driven control schemes, the Zeno behavior can be avoided, and the states of closed-loop systems are globally uniformly ultimately bounded, and the explicit parameter design of the event-driven controllers is proposed.

Notation. If not explicitly stated, matrices in this paper are assumed to have compatible dimensions. \mathbb{R}^n denotes n dimensional Euclidean space. $\mathbb{R}^{m \times n}$ is a set of all $m \times n$ real matrices. $\|\cdot\|$ means the 2-norm of vectors and matrices. For any matrix A , $\lambda(A)$ denotes the eigenvalue of matrix A . Inequality $M > N$ means that matrix $M - N$ is positive definite. Then, $\sup\{\cdot\}$ denotes the supremum of set $\{\cdot\}$, and $\text{diag}\{a, b, c\}$ is a diagonal matrix with a, b, c as main diagonal elements.

2 Problem statement

A linear time-invariant (LTI) plant is considered with event-driven control inputs in the following:

$$\dot{x}(t) = Ax(t) + Bu(t_k), \quad y(t) = Cx(t), \quad t \in [t_k, t_{k+1}), \quad k \in \mathbb{N}, \quad (1)$$

where $x(t) \in \mathbb{R}^n$ represents the state vector, $u(t) \in \mathbb{R}^m$ denotes the control input, $y(t) \in \mathbb{R}^q$ is the measured output, and A, B, C are the system matrices with appropriate dimensions. The transmitting instants $\{t_k\}_{k \in \mathbb{N}}$ are defined as an increasing sequence of positive scalars with $\bigcup_{k \in \mathbb{N}} [t_k, t_{k+1}) = [0, +\infty)$ holding, and $\{t_k\}_{k \in \mathbb{N}}$ are determined by a predefined event-driven scheduler. To hold the control signal continuous, a ZOH is embedded, and thus, during the inter-scheduling interval $[t_k, t_{k+1})$, $u(t) \equiv u(t_k)$.

In this paper, we consider that only the output variables of the physical system can be obtained online. Then the DOF control problem for system (1) is researched in Sections 3 and 4, and three main problems are aimed to be addressed as follows:

(1) How to design output feedback controllers for system (1) with either continuous or sampled output measurements?

(2) How to exclude the Zeno behavior by determining the transmitting instants $\{t_k\}_{k \in \mathbb{N}}$?

(3) For the closed-loop systems, how to analyze the stability with the designed transmitting instants?

3 Control of systems with continuous output measurements

In this section, by assuming that the continuous output measurements $y(t)$ are available, we design the DOF controller as

$$\dot{\hat{x}}_c(t) = K_1\hat{x}_c(t) + K_2y(t), \quad u(t) = K_3\hat{x}_c(t) + K_4y(t), \quad (2)$$

where the $\hat{x}_c(t) \in \mathbb{R}^n$ is the controller state, and $K_i, i = 1, 2, 3, 4$, denote the controller parameter matrices to be ascertained. Thus, for $t \in [t_k, t_{k+1})$, the plant and controller can be reorganized as

$$\begin{aligned} \dot{x}(t) &= Ax(t) + Bu(t_k) \\ &= Ax(t) + Bu(t) - Bu(t) + Bu(t_k) \\ &= Ax(t) + BK_3\hat{x}_c(t) + BK_4y(t) - Be(t) \\ &= (A + BK_4C)x(t) + BK_3\hat{x}_c(t) - Be(t), \end{aligned}$$

where $e(t) = u(t) - u(t_k)$ and

$$\dot{\hat{x}}_c(t) = K_1\hat{x}_c(t) + K_2y(t) = K_2Cx(t) + K_1\hat{x}_c(t).$$

Defining an augmented state $\xi(t) = [x^T(t), \hat{x}_c^T(t)]^T$, we arrive at the closed-loop system as

$$\dot{\xi}(t) = \bar{A}\xi(t) + \bar{B}e(t), \quad t \in [t_k, t_{k+1}), \quad (3)$$

where

$$\bar{A} = \begin{bmatrix} A + BK_4C & BK_3 \\ K_2C & K_1 \end{bmatrix}, \quad \bar{B} = \begin{bmatrix} -B \\ 0 \end{bmatrix}.$$

Moreover, the global uniform ultimate bounded stability of closed-loop system (3) is shown in the following theorem.

Theorem 1. For the closed-loop system (3), an event-driven scheduler is designed to determine the transmitting instants as follows:

$$t_{k+1} = \sup \{t > t_k \mid \|e(t)\|^2 \leq \varepsilon + \varrho \|u(t)\|^2\}, \quad \forall k \in \mathbb{N}, \quad (4)$$

where $\varepsilon > 0$ and $\varrho > 0$ are two user-defined parameters. If the following matrix inequality,

$$Q \triangleq \bar{A}^T P + P\bar{A} + P\bar{B}\bar{B}^T P + \varrho\bar{C}^T\bar{C} < 0, \quad (5)$$

holds with $\bar{C} = [K_4C, K_3]$ for a symmetric and positive definite matrix P , then the system (3) gets the global uniform ultimate bounded stability.

Proof. With a symmetric and positive definite matrix $P > 0$ which is a solution of (5), the Lyapunov function candidate is chosen as $V(t) = \xi^T(t)P\xi(t)$ for $t \in [t_k, t_{k+1})$. Then the derivation of $V(t)$ is

$$\begin{aligned} \dot{V}(t) &= \dot{\xi}^T(t)P\xi(t) + \xi^T(t)P\dot{\xi}(t) \\ &= (\bar{A}\xi(t) + \bar{B}e(t))^T P\xi(t) + \xi^T(t)P(\bar{A}\xi(t) + \bar{B}e(t)) \\ &= \xi^T(t)(\bar{A}^T P + P\bar{A})\xi(t) + e^T(t)\bar{B}^T P\xi(t) + \xi^T(t)P\bar{B}e(t) \\ &= \xi^T(t)(\bar{A}^T P + P\bar{A} + P\bar{B}\bar{B}^T P)\xi(t) - \|e(t) - \bar{B}^T P\xi(t)\|^2 + \|e(t)\|^2. \end{aligned}$$

It can be seen that, with the transmitting instants defined in (4), $\|e(t)\|^2 \leq \varepsilon + \varrho\|u(t)\|^2$ always holds for $t \in [t_k, t_{k+1})$. Hence, for $\forall t \in [t_k, t_{k+1})$, we have

$$\begin{aligned} \dot{V}(t) &\leq \xi^T(t)(\bar{A}^T P + P\bar{A} + P\bar{B}\bar{B}^T P)\xi(t) + \|e(t)\|^2 \\ &= \xi^T(t)(\bar{A}^T P + P\bar{A} + P\bar{B}\bar{B}^T P + \varrho\bar{C}^T\bar{C})\xi(t) + \varepsilon \end{aligned}$$

$$\begin{aligned} &\leq -\frac{\lambda_{\min}(-Q)}{\lambda_{\max}(P)}\xi^T(t)P\xi(t) + \varepsilon \\ &= -\delta V(t) + \varepsilon, \end{aligned} \tag{6}$$

where $\delta = \frac{\lambda_{\min}(-Q)}{\lambda_{\max}(P)}$. From inequality (6), we obtain that the Lyapunov function $V(t)$ will decay in each time interval $[t_k, t_{k+1})$. By the comparison lemma in [5], inequality (6) is obtained as

$$\begin{aligned} V(t) &\leq e^{-\delta t}V(0) + \int_0^t e^{-\delta(t-s)}\varepsilon ds \\ &= e^{-\delta t}\left(V(0) - \frac{\varepsilon}{\delta}\right) + \frac{\varepsilon}{\delta}, \end{aligned}$$

which leads to

$$\begin{aligned} V(t) &\leq e^{-\delta(t-t_k)}V(t_k) + \int_{t_k}^t e^{\delta(t-s)}\varepsilon ds \\ &= e^{-\delta(t-t_k)}V(t_k) + \frac{\varepsilon}{\delta}\left(1 - e^{-\delta(t-t_k)}\right), \end{aligned}$$

implying

$$\begin{aligned} \|\xi(t)\| &\leq \sqrt{\frac{\lambda_{\max}(P)}{\lambda_{\min}(P)}e^{-\delta(t-t_k)}\|\xi(t_k)\|^2 + \frac{\varepsilon(1 - e^{-\delta(t-t_k)})}{\delta\lambda_{\min}(P)}} \\ &\leq \sqrt{\frac{\lambda_{\max}(P)}{\lambda_{\min}(P)}\|\xi(t_k)\|^2 + \frac{\varepsilon}{\delta\lambda_{\min}(P)}}. \end{aligned} \tag{7}$$

Therefore, the closed-loop system (3) can arrive at the global uniform ultimate bounded as inequality $Q < 0$ holds, which completes the proof.

For avoidance of the Zeno behavior, in the next, it will be shown that a positive lower bound of the minimum inter-scheduling interval $t_{\min} \triangleq \min_{k \in \mathbb{N}}\{t_{k+1} - t_k\}$ always exists for the event-driven strategy.

Theorem 2. In the closed-loop system (3), for the minimum inter-scheduling interval t_{\min} , there always exists a positive lower bound $t_{\min}^l > 0$ which satisfies $t_{\min} \geq t_{\min}^l > 0$, with the transmitting instants determined by (4).

Proof. For $\forall k \in \mathbb{N}$, let t_k be an arbitrary transmitting instant. Note that $u(t_k)$ is constant in the time interval $[t_k, t_{k+1})$. Then, for $t \in [t_k, t_{k+1})$, according to the definition of $e(t)$, we have

$$\begin{aligned} \dot{e}(t) &= K_3\dot{\hat{x}}_c(t) + K_4C\dot{x}(t) \\ &= K_3K_1\hat{x}_c(t) + K_3K_2Cx(t) + K_4CAx(t) + K_4CBu(t) - K_4CBu(t_k) + K_4CBu(t_k) \\ &= K_4CBe(t) + (K_3K_2C + K_4CA)x(t) + K_3K_1\hat{x}_c(t) + K_4CBK_4Cx(t_k) + K_4CBK_3\hat{x}_c(t_k) \\ &= \Sigma_1e(t) + \Sigma_2\xi(t) + \Sigma_3\xi(t_k), \end{aligned}$$

where $\Sigma_1 = K_4CB$, $\Sigma_2 = [K_3K_2C + K_4CA \ K_3K_1]$, $\Sigma_3 = [K_4CBK_4C \ K_4CBK_3]$. Moreover, we have

$$\begin{aligned} e(t) &= e^{\Sigma_1(t-t_k)}e(t_k) + \int_{t_k}^t e^{\Sigma_1(t-s)}(\Sigma_2\xi(s) + \Sigma_3\xi(t_k)) ds \\ &= \int_{t_k}^t e^{\Sigma_1(t-s)}(\Sigma_2\xi(s) + \Sigma_3\xi(t_k)) ds. \end{aligned} \tag{8}$$

Define

$$\psi(t_k) = \sqrt{\frac{\lambda_{\max}(P)}{\lambda_{\min}(P)}\|\xi(t_k)\|^2 + \frac{\varepsilon}{\delta\lambda_{\min}(P)}}.$$

Then, it follows from (7) and (8) that

$$\begin{aligned} \|e(t)\| &= \left\| \int_{t_k}^t e^{\Sigma_1(t-s)} (\Sigma_2 \xi(s) + \Sigma_3 \xi(t_k)) \, ds \right\| \\ &\leq \int_{t_k}^t e^{\|\Sigma_1\|(t-s)} (\|\Sigma_2\| \|\xi(s)\| + \|\Sigma_3\| \|\xi(t_k)\|) \, ds. \end{aligned}$$

If $\|\Sigma_1\| \neq 0$, we have

$$\|e(t)\| \leq \frac{\|\Sigma_2\| \|\psi(t_k)\| + \|\Sigma_3\| \|\xi(t_k)\|}{\|\Sigma_1\|} \left(e^{\|\Sigma_1\|(t-t_k)} - 1 \right).$$

Note that the next transmission will not happen before $\|e(t)\|^2 = \varepsilon + \varrho \|u(t)\|^2$ according to the definition of transmitting instants (4). Therefore, the lower bound on the inter-scheduling interval t_{\min}^l can be determined by

$$\frac{\|\Sigma_2\| \|\psi(t_k)\| + \|\Sigma_3\| \|\xi(t_k)\|}{\|\Sigma_1\|} \left(e^{\|\Sigma_1\| t_{\min}^l} - 1 \right) = \sqrt{\varepsilon + \varrho \xi^T(t) \bar{C}^T \bar{C} \xi(t)} \geq \sqrt{\varepsilon},$$

which means that

$$e^{\|\Sigma_1\| t_{\min}^l} \geq 1 + \frac{\sqrt{\varepsilon}}{\Delta(t_k)},$$

where $\Delta(t_k) = \frac{\|\Sigma_2\| \|\psi(t_k)\| + \|\Sigma_3\| \|\xi(t_k)\|}{\|\Sigma_1\|}$. Note that conditions $\|\Sigma_1\| > 0$ and $\frac{\sqrt{\varepsilon}}{\Delta(t_k)} > 0$ hold, which indicates that for any given transmitting instant t_k , $t_{\min}^l > 0$ always holds.

If $\|\Sigma_1\| = 0$, we have

$$\|e(t)\| \leq (t - t_k) (\|\Sigma_2\| \|\psi(t_k)\| + \|\Sigma_3\| \|\xi(t_k)\|).$$

As aforementioned before, because the next transmission will not happen before $\|e(t)\|^2 = \varepsilon + \varrho \|u(t)\|^2$, the lower bound on the inter-scheduling interval t_{\min}^l can be determined by

$$t_{\min}^l (\|\Sigma_2\| \|\psi(t_k)\| + \|\Sigma_3\| \|\xi(t_k)\|) = \sqrt{\varepsilon + \varrho \xi^T(t) \bar{C}^T \bar{C} \xi(t)},$$

which means that

$$t_{\min}^l (\|\Sigma_2\| \|\psi(t_k)\| + \|\Sigma_3\| \|\xi(t_k)\|) \geq \sqrt{\varepsilon},$$

which also implies that $t_{\min}^l > 0$.

From the above discussion, a positive lower bound of the minimum inter-scheduling interval always exists, which completes the proof.

Combining with the stability condition proposed in Theorem 1, a solution of the controller parameters K_1, K_2, K_3 and K_4 is presented in the following theorem.

Theorem 3. For system (1) with the event-driven inputs, there always exists a DOF controller which is in the form of (2) such that states of the closed-loop control system (3) are globally uniformly ultimately bounded, if there exist matrices $W, R, L, F, X > 0$ and $Y > 0$, satisfying

$$\begin{bmatrix} \Xi_{11} + \Xi_{11}^T & W + \Xi_{21}^T & -XB & \sqrt{\varrho} C^T R^T \\ * & \Xi_{22} + \Xi_{22}^T & -B & \sqrt{\varrho} F^T \\ * & * & -I & 0 \\ * & * & * & -I \end{bmatrix} < 0 \tag{9}$$

and $I - YX < 0$, where $\Xi_{11} = XA + LC$, $\Xi_{21} = A + BRC$, $\Xi_{22} = AY + BF$.

Furthermore, if the above conditions are satisfied, parameters of the desired DOF controller should be chosen as

$$\begin{aligned} K_1 &= U^{-T}(W - XAY - XBF - LCY + XBRCY)V^{-T}, \\ K_2 &= U^{-T}L - U^{-T}XBR, \quad K_3 = FV^{-T} - RCYV^{-T}, \quad K_4 = R, \end{aligned} \tag{10}$$

where V and U are two any nonsingular matrices satisfying $I - YX = VU$.

Proof. Define matrix $P = T_2T_1^{-1}$, where T_1 and T_2 are given as

$$T_1 = \begin{bmatrix} I & Y \\ 0 & V^T \end{bmatrix}, \quad T_2 = \begin{bmatrix} X & I \\ U & 0 \end{bmatrix},$$

and $YX + VU = I$, and U, V are any nonsingular matrices. It can be verified that

$$T_1^{-1} = \begin{bmatrix} I & -YV^{-T} \\ 0 & V^{-T} \end{bmatrix},$$

and thus

$$P = \begin{bmatrix} X & U^T \\ U & -UYV^{-T} \end{bmatrix}.$$

Note that $YX - I > 0$ holds, thus $VUY = Y(Y^{-1} - X)Y < 0$ and $-UYV^{-T} = -V^{-1}Y(Y^{-1} - X)YV^{-T} > 0$. Moreover, referring to the well-known Schur complement lemma, it is obtained that

$$X - U^T(-UYV^{-T})^{-1}U = X + U^TV^TY^{-1} = Y^{-1} > 0,$$

which implies that $P > 0$.

With the DOF controller parameters $K_i, i = 1, 2, 3, 4$, it can be shown that

$$T_2^T \bar{A} T_1 = \begin{bmatrix} \Xi_{11} & W \\ \Xi_{21} & \Xi_{22} \end{bmatrix}, \quad T_2^T \bar{B} = \begin{bmatrix} -XB \\ -B \end{bmatrix}, \quad T_1^T \bar{C}^T \bar{C} T_1 = \begin{bmatrix} C^T R^T R C & C^T R^T F \\ * & F^T F \end{bmatrix}.$$

Thus, by the Schur complement lemma, the inequality (9) is rewritten as

$$\begin{bmatrix} T_1^T \bar{A}^T T_2 + T_2^T \bar{A} T_1 + \varrho T_1^T \bar{C}^T \bar{C} T_1 & T_2^T \bar{B} \\ \bar{B}^T T_2 & -I \end{bmatrix} < 0.$$

Moreover, notice that

$$\begin{bmatrix} \bar{A}^T P + P \bar{A} + \varrho \bar{C}^T \bar{C} & P \bar{B} \\ \bar{B}^T P & -I \end{bmatrix} = \begin{bmatrix} T_1^{-T} & 0 \\ 0 & I \end{bmatrix} \begin{bmatrix} T_1^T \bar{A}^T T_2 + T_2^T \bar{A} T_1 + \varrho T_1^T \bar{C}^T \bar{C} T_1 & T_2^T \bar{B} \\ \bar{B}^T T_2 & -I \end{bmatrix} \begin{bmatrix} T_1^{-1} & 0 \\ 0 & I \end{bmatrix}.$$

Thus, the inequality (5) holds, and the closed-loop event-driven control system (3) obtains global uniform ultimate bounded stability.

Remark 1. In Theorem 3, it is worth obtaining that all designed conditions are LMIs. By a standard numerical software, it is easy to solve the decision variables $W, R, L, F, X > 0$ and $Y > 0$ in the LMIs. Thus, based on (10), a desired event-driven DOF controller is immediately constructed when these conditions are feasible.

4 Control of systems with sampled output measurements

In this section, we consider that with a constant sampling period $h > 0$, the system output is sampled in periodic. In other words, only the sampled output measurements $y(ih), i \in \mathbb{N}$, are available for controller (2). In such a case, the DOF controller (2) is modified as

$$\begin{aligned} \dot{\hat{x}}_c(t) &= K_1 \hat{x}_c(t) + K_2 \hat{x}_c(ih) + K_3 y(ih), \\ u(t) &= K_4 \hat{x}_c(t) + K_5 \hat{x}_c(ih) + K_6 y(ih), \end{aligned} \tag{11}$$

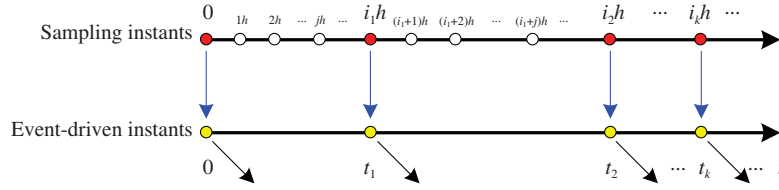


Figure 1 (Color online) Illustration of signal transmission.

where $\hat{x}_c(t) \in \mathbb{R}^n$ denotes the controller state, $\hat{x}_c(ih)$ denotes the controller state at sampled instants and $y(ih)$ denotes the sampled output measurement. In this situation, the controller in (11) will receive the sampled output signal $y(ih)$ at the sampling instant ih , and the $y(ih)$ will be held until next sampling instant $(i+1)h$.

In Section 3, the control input of the plant will be updated at t_k defined in (4). To determine the transmitting instants t_k in (4), the continuous supervision of $e(t)$ is required. As shown in Figure 1, the event-driven scheduler is assumed to work in a discrete manner here, and monitor the control signal $u(t)$ with a constant sampling period h . In this situation, we can determine the transmitting instants by $t_k = i_k h$, where i_k are some integers and $\{i_0, i_1, i_2, \dots\} \subset \{0, 1, 2, 3, \dots\}$ with $i_0 = 0$ and $i_k < i_{k+1}$. To hold the control signal continuous, a ZOH is embedded, and thus $u(t_k)$ will be held during the time-interval $[t_k, t_{k+1})$.

Define $l_{k,j} = (i_k + j)h$, $j = 0, 1, 2, \dots, i_{k+1} - i_k - 1$, which leads to $[t_k, t_{k+1}) = \bigcup_{j=0}^{i_{k+1}-i_k-1} [l_{k,j}, l_{k,j+1})$. Let $\tau(t) = t - l_{k,j}$, which satisfies $0 \leq \tau(t) \leq h$ with $t \in [l_{k,j}, l_{k,j+1})$, obviously. Furthermore, we define $e_\sigma(t) = u(l_{k,j}) - u(i_k h)$, $j = 1, 2, \dots$, and thus $e_\sigma(t)$ is a continuous-from-the-right and piecewise constant function. Above all, the transmitting instant $i_{k+1}h$ can be determined by

$$i_{k+1} = \max_{m \in \mathbb{Z}} \{m > i_k \mid \|e_\sigma(mh)\|^2 \leq \bar{\varepsilon} + \bar{\varrho} \|u(mh)\|^2\}, \quad (12)$$

where $\bar{\varepsilon}$ and $\bar{\varrho}$ are the event-driven parameters chosen in advance. It can be verified that, inequality $\|e_\sigma(t)\|^2 \leq \bar{\varepsilon} + \bar{\varrho} \|u(t)\|^2$ always holds for $t \in [i_k h, i_{k+1} h)$.

For time $t \in [l_{k,j}, l_{k,j+1})$, the plant and controller system can be reorganized as

$$\begin{aligned} \dot{x}(t) &= Ax(t) + Bu(t_k) \\ &= Ax(t) + Bu(l_{k,j}) - Bu(l_{k,j}) + Bu(t_k) \\ &= Ax(t) + B(K_4 + K_5)\hat{x}_c(l_{k,j}) + BK_6 y(l_{k,j}) - Be_\sigma(t) \\ &= Ax(t) + B(K_4 + K_5)\hat{x}_c(t - \tau(t)) + BK_6 Cx(t - \tau(t)) - Be_\sigma(t), \\ \dot{\hat{x}}_c(t) &= K_1 \hat{x}_c(t) + K_2 \hat{x}_c(l_{k,j}) + K_3 y(l_{k,j}) \\ &= K_1 \hat{x}_c(t) + K_2 \hat{x}_c(t - \tau(t)) + K_3 Cx(t - \tau(t)). \end{aligned}$$

Define variable $\xi(t) = [x^T(t), \hat{x}_c^T(t)]^T$. It is easy to obtain a closed-loop system as follows:

$$\dot{\xi}(t) = \tilde{A}\xi(t) + \tilde{A}_d\xi(t - \tau(t)) + \tilde{B}e_\sigma(t), \quad t \in [l_{k,j}, l_{k,j+1}), \quad (13)$$

where

$$\tilde{A} = \begin{bmatrix} A & 0 \\ 0 & K_1 \end{bmatrix}, \quad \tilde{B} = \begin{bmatrix} -B \\ 0 \end{bmatrix}, \quad \tilde{A}_d = \begin{bmatrix} BK_6 C & B(K_4 + K_5) \\ K_3 C & K_2 \end{bmatrix}.$$

Before studying the stability of closed-loop system (13), the following lemma is given in advance.

Lemma 1 ([25]). Let $x(t) : (p, q) \rightarrow \mathbb{R}^n$ be absolutely continuous with $\dot{x}(t) \in \mathcal{L}_2(p, q)$ and $x(p) = 0$, and then inequality

$$\int_p^q x^T(s) M x(s) ds \leq \frac{4(q-p)^2}{\pi^2} \int_p^q \dot{x}^T(s) M \dot{x}(s) ds$$

holds for any $M > 0$.

Motivated by [25], we can arrive at the following results.

Theorem 4. Consider the closed-loop system (13) with transmitting instants determined by

$$t_{k+1} = i_{k+1}h, \tag{14}$$

where i_k is given by (12) and h denotes the sampling period. For a given parameter $\bar{\varrho} > 0$, if there exist matrices $N_1, N_2, P > 0$ and $S > 0$ with appropriate dimensions satisfying the following matrix inequality:

$$\tilde{\Phi} \triangleq \Phi + N^T \tilde{B} \tilde{B}^T N + \bar{\varrho} \tilde{C}^T \tilde{C} < 0, \tag{15}$$

where

$$\Phi = \begin{bmatrix} \Phi_1 & P - N_1^T + (\tilde{A} + \tilde{A}_d)^T N_2 & -N_1^T \tilde{A}_d \\ * & h^2 S - N_2 - N_2^T & -N_2^T \tilde{A}_d \\ * & * & -\frac{\pi^2}{4} S \end{bmatrix},$$

$$\tilde{C} = [K_6 C \ K_4 + K_5 \ 0 \ 0 \ -K_6 C \ -K_5], \quad N = [N_1 \ N_2 \ 0],$$

with $\Phi_1 = N_1^T (\tilde{A} + \tilde{A}_d) + (\tilde{A} + \tilde{A}_d)^T N_1$, then system (13) obtains the global uniform ultimate bounded stability.

Proof. Consider the following Lyapunov functional for $t \in [l_{k,j}, l_{k,j+1})$,

$$V(t) = \xi^T(t) P \xi(t) + h^2 \int_{t-\tau(t)}^t \dot{\xi}^T(s) S \dot{\xi}(s) ds - \frac{\pi^2}{4} \int_{t-\tau(t)}^t \nu^T(s) S \nu(s) ds,$$

where $P > 0, S > 0$ and $\nu(t) = \xi(t) - \xi(t - \tau(t))$. It turns out that $\dot{\tau}(t) = 1, \dot{\xi}(t - \tau(t)) = 0$, and thus $\dot{\nu}(t) = \dot{\xi}(t)$. By using the Wirtinger inequality, $V(t) \geq 0$ is solved, and the last two terms in $V(t)$ vanish at $t = l_{k,j}$, i.e., $V(l_{k,j}) = \xi^T(l_{k,j}) P \xi(l_{k,j})$. Hence, condition $\lim_{t \rightarrow l_{k,j}} V(t) \geq V(l_{k,j})$ holds.

Differentiating $V(t)$ along system (13), we have

$$\dot{V}(t) = 2\xi^T(t) P \dot{\xi}(t) + h^2 \dot{\xi}^T(t) S \dot{\xi}(t) - \frac{\pi^2}{4} \nu^T(t) S \nu(t),$$

which together with the fact

$$2(\xi^T(t) N_1^T + \dot{\xi}^T(t) N_2^T) ((\tilde{A} + \tilde{A}_d) \xi(t) - \tilde{A}_d \nu(t) + \tilde{B} e_\sigma(t) - \dot{\xi}(t)) = 0$$

gives that

$$\dot{V}(t) \leq \eta^T(t) \Phi \eta(t) + 2(\xi^T(t) N_1^T + \dot{\xi}^T(t) N_2^T) \tilde{B} e_\sigma(t),$$

where $\eta(t) = [\xi^T(t), \dot{\xi}^T(t), \nu^T(t)]^T$. Note that

$$2(\xi^T(t) N_1^T + \dot{\xi}^T(t) N_2^T) \tilde{B} e_\sigma(t) \leq \eta^T(t) \begin{bmatrix} N_1^T \\ N_2^T \\ 0 \end{bmatrix} \tilde{B} \tilde{B}^T [N_1 \ N_2 \ 0] \eta(t) + \|e_\sigma(t)\|^2,$$

which together with $\|e_\sigma(t)\|^2 \leq \bar{\varepsilon} + \bar{\varrho} \eta^T(t) \tilde{C}^T \tilde{C} \eta(t)$ yields

$$\dot{V}(t) \leq \eta^T(t) \tilde{\Phi} \eta(t) + \bar{\varepsilon}. \tag{16}$$

Thus, states of the closed-loop system (13) are shown to be globally uniformly ultimately bounded, which completes the proof.

With the stability condition presented in Theorem 4, the following theorem presents a solution of the sampled output controller parameters $K_i, i = 1, 2, 3, 4, 5, 6$.

Theorem 5. For system (1) with event-driven inputs, there exists a dynamic sampled output controller in the form of (11) such that the closed-loop control system (13) obtains the global uniformly ultimate bounded stability, if there exist matrices $W, R, L, F, H, Z, X > 0$ and $Y > 0$ satisfying

$$\begin{bmatrix} \Lambda_{11} & \Lambda_{12} & \Lambda_{13} \\ * & \Lambda_{22} & \Lambda_{23} \\ * & * & \Lambda_{33} \end{bmatrix} < 0 \tag{17}$$

and $I - YX < 0$, where

$$\begin{aligned} \Lambda_{11} &= \begin{bmatrix} \Xi_{11} + \Xi_{11}^T & H + \Xi_{21}^T \\ * & \Xi_{22} + \Xi_{22}^T \end{bmatrix}, \quad \Lambda_{12} = \begin{bmatrix} \Xi_{11}^T & \Xi_{21}^T & -LC & -W \\ H^T & \Xi_{22}^T & -BRC & -BF \end{bmatrix}, \\ \Lambda_{13} &= \begin{bmatrix} -XB & \sqrt{\bar{\rho}}C^T R^T \\ -B & \sqrt{\bar{\rho}}F^T \end{bmatrix}, \quad \Lambda_{22} = \begin{bmatrix} (h^2 - 2)X & (h^2 - 2)I & -LC & -W \\ * & (h^2 - 2)Y & -BRC & -BF \\ * & * & -\frac{\pi^2}{4}X & -\frac{\pi^2}{4}I \\ * & * & * & -\frac{\pi^2}{4}Y \end{bmatrix}, \\ \Lambda_{23} &= \begin{bmatrix} -XB & 0 \\ -B & 0 \\ 0 & \sqrt{\bar{\rho}}C^T R^T \\ 0 & \sqrt{\bar{\rho}}Z^T \end{bmatrix}, \quad \Lambda_{33} = \begin{bmatrix} -I & 0 \\ * & -I \end{bmatrix}, \end{aligned}$$

with $\Xi_{11} = XA + LC$, $\Xi_{21} = A + BRC$ and $\Xi_{22} = AY + BF$.

Furthermore, if the above conditions are satisfied, parameters of the desired DOF controller can be chosen as

$$\begin{aligned} K_1 &= U^{-T}(H - W - XAY)V^{-T}, \\ K_2 &= U^{-T}(W - XBF - LCY + XBRCY)V^{-T}, \\ K_3 &= U^{-T}(L - XBR), \quad K_4 = (F - Z)V^{-T}, \\ K_5 &= (Z - RCY)V^{-T}, \quad K_6 = R, \end{aligned} \tag{18}$$

where V and U are any nonsingular matrices satisfying $VU = YX + I$.

Proof. With the same definitions for T_1 and T_2 in the proof of Theorem 3, letting $P = S = N_1 = N_2 = T_2T_1^{-1}$, we can arrive at conditions $P > 0$ and $S > 0$. Moreover, with the dynamic sampled output feedback controller parameters $K_i, i = 1, 2, 3, 4, 5, 6$, it can be obtained that

$$\begin{aligned} T_2^T(\tilde{A} + \tilde{A}_d)T_1 &= \begin{bmatrix} XA + LC & H \\ A + BRC & AY + BF \end{bmatrix}, \quad T_2^T\tilde{A}_dT_1 = \begin{bmatrix} LC & W \\ BRC & BF \end{bmatrix}, \\ T_1^TT_2 &= T_2^TT_1 = \begin{bmatrix} X & I \\ I & Y \end{bmatrix}, \quad T_2^T\tilde{B} = \begin{bmatrix} -XB \\ -B \end{bmatrix}, \\ \tilde{C}_1T_1 &= \begin{bmatrix} RC & F \end{bmatrix}, \quad \tilde{C}_3T_1 = \begin{bmatrix} -RC & -Z \end{bmatrix}, \end{aligned}$$

where $\tilde{C}_1 = [K_6C \ K_4 + K_5]$ and $\tilde{C}_3 = [-K_6C \ -K_5]$. With the using of Schur complement, inequality (15) can be rewritten as

$$\tilde{\Phi} = \begin{bmatrix} N_1^T(\tilde{A} + \tilde{A}_d) + (\tilde{A} + \tilde{A}_d)^TN_1 & P - N_1^T + (\tilde{A} + \tilde{A}_d)^TN_2 & -N_1^T\tilde{A}_d & N_1^T\tilde{B} & \sqrt{\bar{\rho}}\tilde{C}_1^T \\ * & h^2S - N_2 - N_2^T & -N_2^T\tilde{A}_d & N_2^T\tilde{B} & 0 \\ * & * & -\frac{\pi^2}{4}S & 0 & \sqrt{\bar{\rho}}\tilde{C}_3^T \\ * & * & * & -I & 0 \\ * & * & * & * & -I \end{bmatrix} < 0.$$

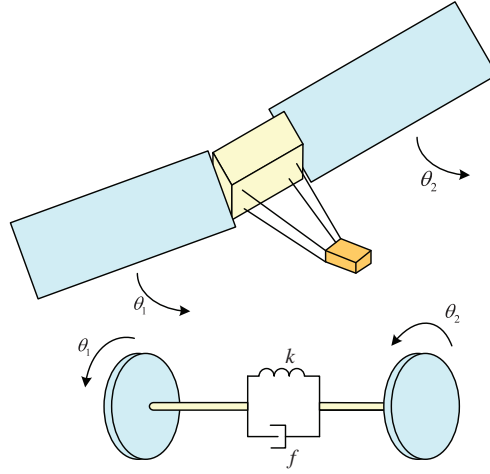


Figure 2 (Color online) The satellite system.

Then, we have

$$\tilde{\Phi} = \text{diag}\{T_1^{-T}, T_1^{-T}, T_1^{-T}, I, I\} \bar{\Phi} \text{diag}\{T_1^{-1}, T_1^{-1}, T_1^{-1}, I, I\},$$

where

$$\bar{\Phi} = \begin{bmatrix} T_2^T(\tilde{A} + \tilde{A}_d)T_1 + T_1^T(\tilde{A} + \tilde{A}_d)^T T_2 & T_1^T(\tilde{A} + \tilde{A}_d)^T T_2 & -T_2^T \tilde{A}_d T_1 & T_2^T \tilde{B} & \sqrt{\tilde{\varrho}} T_1^T \tilde{C}_1^T \\ * & (h^2 - 2)T_1^T T_2 & -T_2^T \tilde{A}_d T_1 & T_2^T \tilde{B} & 0 \\ * & * & -\frac{\pi^2}{4} T_1^T T_2 & 0 & \sqrt{\tilde{\varrho}} T_1^T \tilde{C}_3^T \\ * & * & * & -I & 0 \\ * & * & * & * & -I \end{bmatrix} < 0.$$

Thus, inequality (17) is obtained, and the closed-loop control system (13) gets the global uniformly ultimate bounded stability, which completes the proof.

Remark 2. Note that the structure of the dynamic sampled output feedback controller (11) is different from the DOF controller (2). Because there must exist two nonlinear terms in (17) which is arrived from condition (15) when the form of dynamic sampled output feedback controller is taken as (2), we redesign the dynamic sampled output feedback controller (11) for the solvable LMI condition (17) by introducing two terms of the controller state $\hat{x}_c(ih)$ in this paper. This method will be shown to be effective for a closed-loop system with the dynamic sampled output feedback control by an illustrative simulation in the following.

Remark 3. In Theorem 5, the LMI condition (17) is satisfied over the decision variables $X > 0$, $Y > 0$, W , R , L , F , H and Z . Moreover, by solving the conditions in Theorem 5 via a standard numerical software, parameters of the desired dynamic sampled output feedback controller (11) can be received based on (18).

5 Illustrative example

In this section, the proposed control approaches will be applied to a satellite system, whose sketch is shown as Figure 2.

For the convenience of analysis, the state vector is chosen as $x(t) = [\theta_1^T(t) \ \theta_2^T(t) \ \dot{\theta}_1^T(t) \ \dot{\theta}_2^T(t)]^T$, where $\theta_1(t)$ and $\theta_2(t)$ denote the yaw angles for the main body and the instrumentation module, respectively.

According to [26], the state-space representation of the satellite system can be linearized as

$$\dot{x}(t) = \begin{bmatrix} 0 & 0 & 1 & 0 \\ 0 & 0 & 0 & 1 \\ -0.09 & 0.09 & -0.04 & 0.04 \\ 0.09 & -0.09 & 0.04 & -0.04 \end{bmatrix} x(t) + \begin{bmatrix} 0 \\ 0 \\ 1 \\ 0 \end{bmatrix} u(t),$$

$$y(t) = \begin{bmatrix} 0 & 1 & 0 & 0 \end{bmatrix} x(t).$$

The initial state $x(0)$ is assumed as $[0.2 \ 0.3 \ -0.3 \ -0.2]^T$, and then event-driven parameters are given as $\sqrt{\varepsilon} = 0.005$ and $\sqrt{\varrho} = 0.005$. From Theorem 3, the controller parameter matrices K_1, K_2, K_3 and K_4 can be computed as

$$K_1 = \begin{bmatrix} 50.3502 & 2.8629 & 28.1404 & 5.9067 \\ -50.6963 & -2.967 & -31.179 & -5.0432 \\ -80.7737 & -4.5354 & -44.266 & -9.5086 \\ -107.8983 & -7.2436 & -58.7651 & -13.2154 \end{bmatrix},$$

$$K_2 = \begin{bmatrix} 1.2551 & -17.8524 & 1.2157 & -37.7471 \end{bmatrix}^T,$$

$$K_3 = \begin{bmatrix} -80.6856 & 4.5995 & 43.4514 & 9.5605 \end{bmatrix},$$

$$K_4 = \begin{bmatrix} -0.1168 \end{bmatrix}.$$

Thus, the simulation results are shown in Figures 3 and 4. Figure 3 shows the state responses of the closed-loop system with the traditional continuous-time control scheme and proposed event-driven control scheme. It can be seen that the performance of the system with event-driven control scheme is almost same as that of the traditional continuous-time control one, and the states of the closed-loop system are globally uniformly ultimately bounded. Furthermore, the error signal $\|e(t)\|$ and inter-scheduling intervals are shown in Figure 4. It turns out from Figure 4 that the communication frequency can be highly reduced for the closed-loop system with an event-driven DOF controller. Especially, the control signals are scarcely transmitted when the closed-loop system gets the global uniformly ultimate bounded stability.

The simulation results of the proposed event-driven control approach will be shown for the system with sampled outputs in the following.

Take the sampling period $h = 0.015$ s. The initial state $x(0)$ is also assumed as $[0.2 \ 0.3 \ -0.3 \ -0.2]^T$, and then event-driven parameters are given by $\sqrt{\varepsilon} = 0.001$ and $\sqrt{\varrho} = 0.01$. From Theorem 5, the controller parameter matrices $K_i, i = 1, 2, 3, 4, 5, 6$ can be computed as

$$K_1 = \begin{bmatrix} -0.3721 & 0.0769 & 0.9076 & -0.0577 \\ 9.5757 & 2.2631 & 1.577 & 2.0642 \\ -0.4246 & 0.0074 & -1.0244 & 0.006 \\ -2.2813 & -2.0573 & -4.5547 & -0.9468 \end{bmatrix},$$

$$K_2 = \begin{bmatrix} 6.4422 & -0.022 & 3.2386 & 0.6606 \\ -6.072 & -2.3385 & 0.7294 & -1.5865 \\ -8.4414 & -0.0294 & -4.1502 & -0.8894 \\ -27.8418 & 1.0270 & -15.4902 & -2.4742 \end{bmatrix},$$

$$K_3 = \begin{bmatrix} -1.9098 & -5.1231 & 2.3316 & 10.9882 \end{bmatrix}^T,$$

$$K_4 = \begin{bmatrix} 3.5304 & 0.3441 & 1.2059 & 0.5074 \end{bmatrix},$$

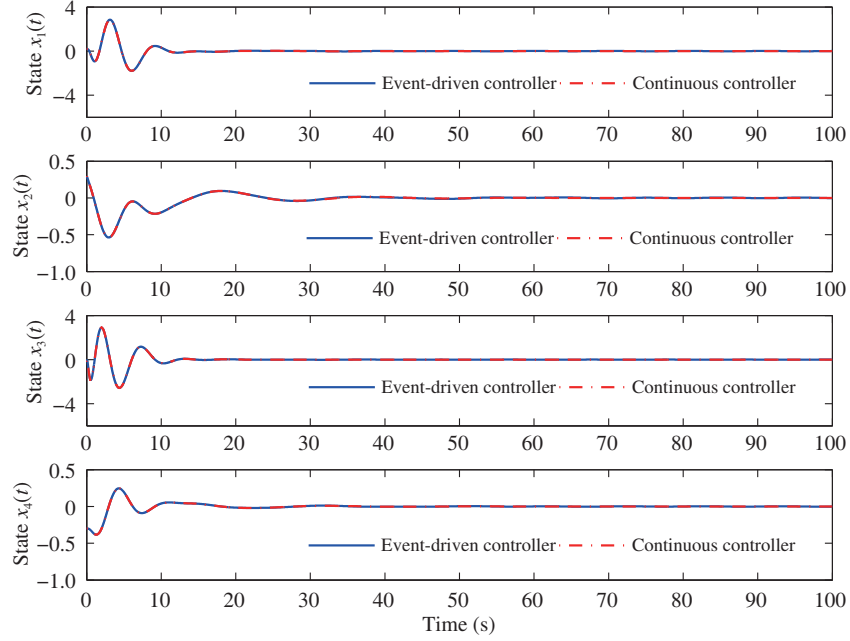


Figure 3 (Color online) State responses: continuous controller and event-driven controller (continuous outputs case).

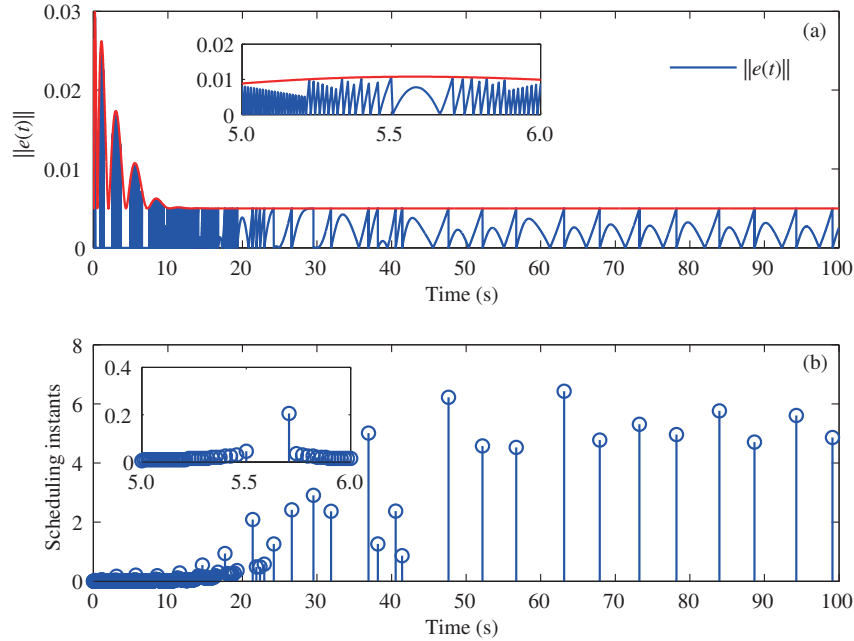


Figure 4 (Color online) (a) State error $\|e(t)\|$ and (b) the corresponding inter-scheduling intervals (continuous outputs case).

$$K_5 = \begin{bmatrix} 5.105 & -0.3181 & 3.0463 & 0.4008 \end{bmatrix},$$

$$K_6 = \begin{bmatrix} -2.3973 \end{bmatrix}.$$

Then, the simulation results are shown in Figures 5 and 6. Obviously, with the designed dynamic sampled output feedback controller (11), the states of the closed-loop system are globally uniformly ultimately bounded. Furthermore, the controller rarely triggers as the closed-loop system runs in a stable state meanwhile the controller performance can also be guaranteed, and the effectiveness of the proposed event-driven control approach is illustrated ultimately.

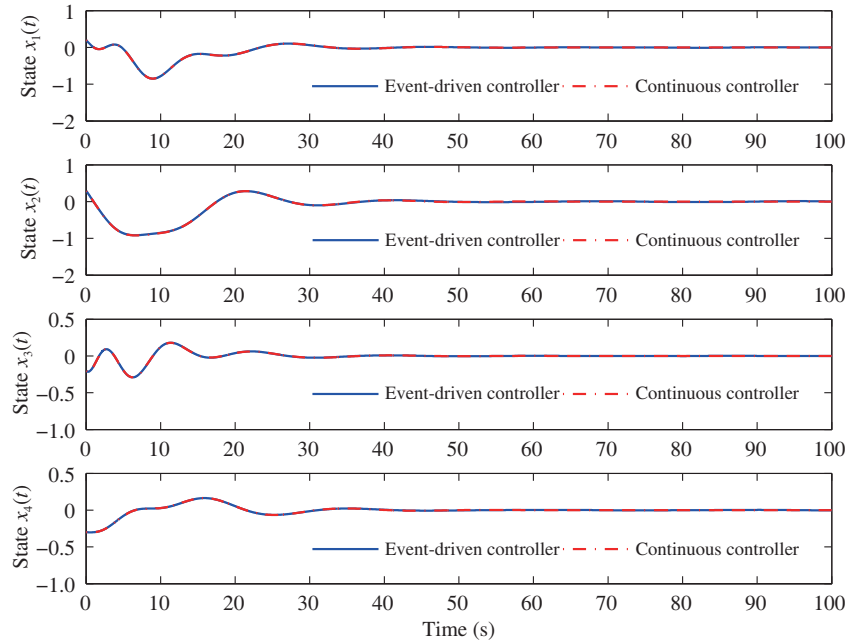


Figure 5 (Color online) State responses: continuous controller and event-driven controller (sampled outputs case).

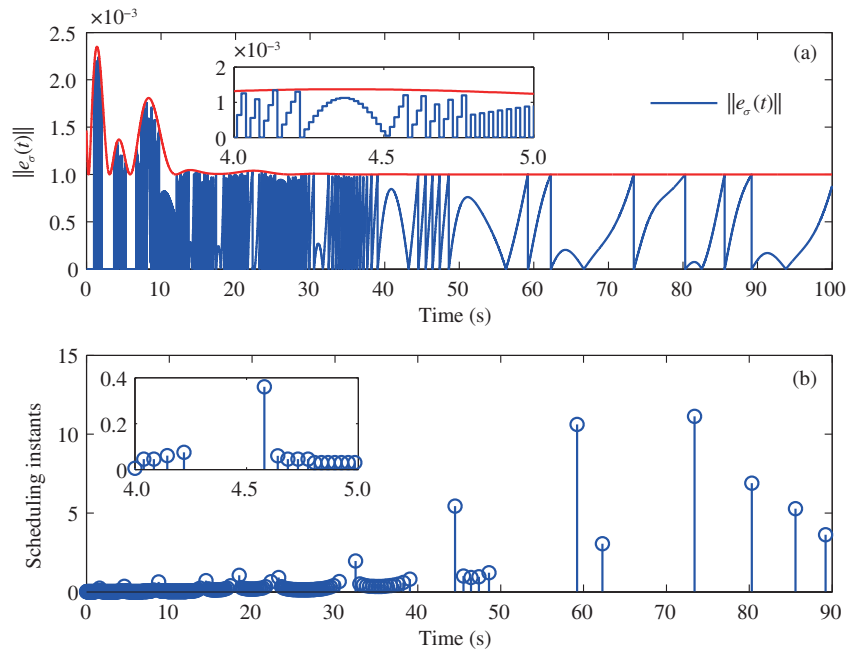


Figure 6 (Color online) (a) State error $\|e_\sigma(t)\|$ and (b) the corresponding inter-scheduling intervals (sampled outputs case).

6 Conclusion

This paper has investigated the problem of DOF control on systems with event-driven control inputs, and the control schemes have been proposed for systems with continuous and sampled output measurements, respectively. The event-driven instants and the controller parameters have been designed with the avoidance of the Zeno behavior. It has been illustrated that with the designed event-driven scheduler, states of the resulting closed-loop system are uniformly ultimately bounded. A numerical example has been provided to explain the applicability of developed results in the end.

Acknowledgements This work was supported by National Natural Science Foundation of China (Grant Nos. 61873030, 61603041), National Natural Science Foundation Projects of International Cooperation and Exchanges (Grant No. 61720106-010), and Foundation for Innovative Research Groups of the National Natural Science Foundation of China (Grant No. 61621063). The authors would like to thank the anonymous reviewers for their detailed comments which helped to improve the quality of the paper.

References

- 1 Hu L, Wang Z D, Han Q L, et al. State estimation under false data injection attacks: security analysis and system protection. *Automatica*, 2018, 87: 176–183
- 2 Zou L, Wang Z D, Han Q L, et al. Ultimate boundedness control for networked systems with try-once-discard protocol and uniform quantization effects. *IEEE Trans Automat Control*, 2017, 62: 6582–6588
- 3 Yan H C, Zhang H, Zhan X S, et al. Event-based H_∞ fault detection for buck converter with multiplicative noises over network. *IEEE Trans Circ Syst I*, 2019, 66: 2361–2370
- 4 Wu X T, Shi P, Tang Y, et al. Input-to-state stability of nonlinear stochastic time-varying systems with impulsive effects. *Int J Robust Nonlin Control*, 2017, 27: 1792–1809
- 5 Zhang J H, Lin Y J, Shi P. Output tracking control of networked control systems via delay compensation controllers. *Automatica*, 2015, 57: 85–92
- 6 Yan H C, Xu X L, Zhang H, et al. Distributed event-triggered H_∞ state estimation for T-S fuzzy systems over filtering networks. *J Franklin Inst*, 2017, 354: 3760–3779
- 7 Li Y Z, Shi D W, Chen T W. False data injection attacks on networked control systems: a stackelberg game analysis. *IEEE Trans Automat Control*, 2018, 63: 3503–3509
- 8 Tan C, Zhang H S. Necessary and sufficient stabilizing conditions for networked control systems with simultaneous transmission delay and packet dropout. *IEEE Trans Automat Control*, 2017, 62: 4011–4016
- 9 Li Y J, Liu G P, Sun S L, et al. Prediction-based approach to finite-time stabilization of networked control systems with time delays and data packet dropouts. *Neurocomputing*, 2019, 329: 320–328
- 10 Zhang J H, Feng G. Event-driven observer-based output feedback control for linear systems. *Automatica*, 2014, 50: 1852–1859
- 11 Zhang X M, Han Q L, Zhang B L. An overview and deep investigation on sampled-data-based event-triggered control and filtering for networked systems. *IEEE Trans Ind Inf*, 2017, 13: 4–16
- 12 Yu Y G, Zeng Z W, Li Z K, et al. Event-triggered encirclement control of multi-agent systems with bearing rigidity. *Sci China Inf Sci*, 2017, 60: 110203
- 13 Huang N, Duan Z S, Zhao Y. Distributed consensus for multiple Euler-Lagrange systems: an event-triggered approach. *Sci China Tech Sci*, 2016, 59: 33–44
- 14 Wang J, Zhang X M, Lin Y F, et al. Event-triggered dissipative control for networked stochastic systems under non-uniform sampling. *Inf Sci*, 2018, 447: 216–228
- 15 Li T F, Fu J, Deng F, et al. Stabilization of switched linear neutral systems: an event-triggered sampling control scheme. *IEEE Trans Automat Control*, 2018, 63: 3537–3544
- 16 Borgers D P, Dolk V S, Heemels W P M H. Riccati-based design of event-triggered controllers for linear systems with delays. *IEEE Trans Automat Control*, 2018, 63: 174–188
- 17 Gu Z, Shi P, Yue D. An adaptive event-triggering scheme for networked interconnected control system with stochastic uncertainty. *Int J Robust Nonlin Control*, 2017, 27: 236–251
- 18 Yan H C, Wang T T, Zhang H, et al. Event-triggered H_∞ control for uncertain networked T-S fuzzy systems with time delay. *Neurocomputing*, 2015, 157: 273–279
- 19 Liu R J, She J H, Wu M, et al. Robust disturbance rejection for a fractional-order system based on equivalent-input-disturbance approach. *Sci China Inf Sci*, 2018, 61: 070222
- 20 Zhang X M, Han Q L. Event-triggered dynamic output feedback control for networked control systems. *IET Control Theor Appl*, 2014, 8: 226–234
- 21 Li H C, Zuo Z Q, Wang Y J. Dynamic output feedback control for systems subject to actuator saturation via event-triggered scheme. *Asian J Control*, 2018, 20: 207–215
- 22 Guo Y, Lin C, Chen B, et al. Necessary and sufficient conditions for the dynamic output feedback stabilization of fractional-order systems with order $0 < \alpha < 1$. *Sci China Inf Sci*, 2019, 62: 199201
- 23 Wang Y J, Jia Z X, Zuo Z Q. Dynamic event-triggered and self-triggered output feedback control of networked switched linear systems. *Neurocomputing*, 2018, 314: 39–47
- 24 Gu Z, Huan Z, Yue D, et al. Event-triggered dynamic output feedback control for networked control systems with probabilistic nonlinearities. *Inf Sci*, 2018, 457–458: 99–112
- 25 Liu K, Fridman E. Wirtinger’s inequality and Lyapunov-based sampled-data stabilization. *Automatica*, 2012, 48: 102–108
- 26 Gao H J, Meng X Y, Chen T W, et al. Stabilization of networked control systems via dynamic output-feedback controllers. *SIAM J Control Opt*, 2010, 48: 3643–3658